OBJECTIVE METHOD OF MEASURING RESOLUTION OF IMAGE INTENSIFIER TUBES

Krzysztof Chrzanowski[1,2], Bolesław Stafiej[2]

1) Military University of Technology, Institute of Optoelectronics, 2 Kaliskiego Str., 00-908 Warsaw, Poland
2) INFRAMET, Bugaj 29a, Koczargi Nowe, 05-082 Stare Babice, Poland (✉ kch@inframet.com)

Abstract

Image intensifier tubes (IITs) are the most important modules of night vision devices used in huge numbers by military forces worldwide. Resolution is the most important parameter of IITs that presents information about ability of these devices to produce output images preserving information about details of the observed scenery. Despite its importance, it is still a common practice to measure resolution subjectively, by an observer looking at image of a resolution target created by a tested IIT. A series of attempts have been carried out to develop objective methods for accurate resolution measurement of IITs but with limited success. Accuracy of these methods varies depending on the tested IIT. This paper presents detailed analysis of proposed methods for objective resolution measurement. This analysis has shown that significant variability of accuracy of these methods is caused by one main drawback: the methods do not take into account influence of the spatial noise effect on human perception of image of the resolution target. Thus, an improved method taking into account spatial noise and its impact on target detection has been proposed. The method has been validated through experimental verification that shows accuracy improvements compared to other objective methods. This new approach improves accuracy of measurement of resolution of IITs to a level that can be accepted at professional test stations. In this way, this new method has potential to replace the standard subjective method to measure resolution of IITs and fix the biggest flaw of the standard test stations: measurement subjectivity.

Keywords: image intensifier, IIT, resolution measurement, subjective resolution, objective resolution.

1. Introduction

Image intensifier tubes (IITs) are vacuum tubes that amplify a non-detectable (or barely seen) image at their photocathodes to a bright, clearly visible image created at the screen plane. The amplification is a double conversion process. First, the incoming light is converted into photoelectrons by the photocathode of the tube. Then, highly intensified photoelectrons strike the phosphor screen (anode) and a bright image is created that a human can easily see. This makes IITs the most important component of night vision devices used in worldwide in military, security and civilian applications [1].

Resolution is a parameter to quantify the quality of images generated by IITs. It is considered as the most important parameter of IITs [2]. In detail, the resolution is typically defined as a spatial frequency of the smallest resolvable element of the test target that can be resolved by a human observer [3–5]. It is a parameter that is present in practically every data sheet of image intensifier tubes [6–8].

According to this classical subjective measurement method, the observer is looking at a set of progressively smaller elements until he can no longer distinguish finer details of the observed target. The main problem is the subjective nature of such measurements. The results are based solely on the observer's judgment.

A series of attempts have been carried out to develop objective methods for accurate resolution measurement of IITs [9–11], but with limited success. Accuracy of these methods varies depending on the tested IIT.

This paper presents detailed analysis of methods for objective resolution measurement of IITs. The analysis has shown that significant variability of accuracy of these methods is caused by one main drawback: the methods do not take into account the influence of spatial noise effect on human perception of image of the resolution target. In such a situation, an improved method that takes into account spatial noise and its impact on target detection has been proposed. The proposed method has been later validated through experimental verification by comparison tests with the classical subjective method. The obtained results show significant accuracy improvements of the new method compared to the other objective methods.

2. Classical subjective method

Resolution of IITs is typically measured using the subjective method proposed by standards issued by US military authorities [12]. The resolution is defined as the smallest pattern of the *United States Air Force* (USAF) 1951 Resolving Power Test Target (Fig. 1) for which the observer can distinguish three black lines and the clear areas between the black lines, for both the vertical and horizontal direction [3–5]. Technical details of USAF1951 target can be found in [13].
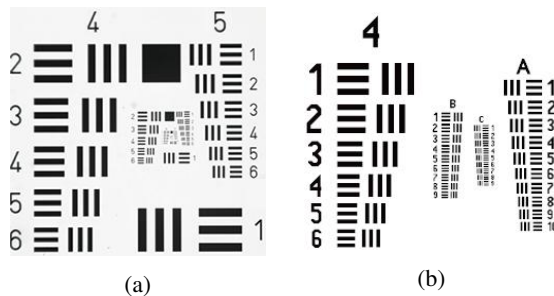

Fig. 1. Drawings of typical resolution targets used in testing IITs: a) typical USAF 1951 resolution target (groups 4-8), b) modified USAF1951 (increased number of patters with a smaller step between them).

This classical method has many known issues, which stems mostly from subjective nature of the measurement. In the classical method, the observer decides whether the pattern is resolvable or not. There is no way to recreate another observer's decision process as every person is different. Further on, the observer's mental state and experience are important as well. Trained observers are capable of resolving higher frequencies. Finally, resolving patterns is a mundane and mentally

exhausting task. A well-rested observer can score higher than a fatigued one and, during a long measurement session, there can be a drop in the resolving ability. As such, observers usually do not work full time, which drives up the cost.

To minimize the drawbacks of the standard method, it is necessary to exclude the observer from the measurement and derive resolution from other parameters that can be measured objectively.

3. Review of objective resolution measurement methods

In the past, there were several attempts to establish an objective method of measuring resolution [9–11]. Here, the following methods are discussed:
1. Maximum output brightness,
2. Fourier transform of bar patterns,
3. MTF threshold.

3.1. Maximum output brightness

Stefanik *et al.* in [9] calculated the resolution of the whole night vision device, or as they called them, image intensifiers systems. They focused primarily on lower light level conditions. However, their methodology can be extrapolated to measurements of IITs with few modifications.

They proposed, based on previous works on pattern recognition, minimum contrast and the temporal signaltonoise threshold factor for the visual discrimination between adjacent areas of the target as a foundation of their model. The resolution is calculated as in (1):

$$R = \frac{C_b}{4 \cdot k \cdot A_0} \sqrt{\frac{S \cdot t \cdot L_0}{(2 - C_b) \cdot q}}, \tag{1}$$

where: C_b is the Weber contrast, L_0 – screen luminance, S – IIT sensitivity, t – eye integration time, k – contrast threshold value, q – electron charge, A_0 – device aperture.

However, since contrast depends on the observed target frequency and resolution is defined as said target frequency, it is more accurate to present (2) as:

$$R = \frac{C_b(R)}{4 \cdot k \cdot A_0} \sqrt{\frac{S \cdot t \cdot L_0}{[2 - C_b(R)] \cdot q}}. \tag{2}$$

Due to relationship between contrast and resolution, (2) cannot be directly used to obtain limiting resolution. However, for that purpose we can rewrite (2) using detection threshold T. Detection threshold is a figure of merit that informs whether the target is recognizable or not. Targets with T greater than 1 can be resolved. Resolution is a spatial frequency for which T is equal to 1. During the resolution measurement, input light is high so we can safely assume that IIT reaches *maximum output brightness* (MOB). We can subside MOB for L_0 in calculation. Stefanik showed that sensitivity S is proportional to IIT signal to noise ratio (SNR) squared. Contrast C_b can be obtained through an MTF measurement. Taken all of these into consideration, we can rewrite (2) to (3). Equation (3) can be used to obtain resolution.

$$T(v) = \frac{1}{k_{\text{IIT}}} \cdot \frac{C_b(\text{MTF})}{\sqrt{[2 - C_b(\text{MTF})]}} \cdot SNR \cdot \sqrt{\text{MOB}}, \tag{3}$$

where: k_{IIT} is a coefficient different from k used in (1).

3.2. Fourier transform of bar patterns

Wang et al in [10] has a more direct approach. They propose to determine the resolution based on the Fourier transform of the middle bar of a 3 bar input image. The process of extracting resolution is as follows. The bar pattern is captured with a high magnification video microscope. Then, an average profile of each target is drawn. From the average profile, the middle bar is selected, multiplied and its spectrum calculated. The *highest peak amplitude* (HPA) of the spectrogram is compared with a threshold and if it is higher, then pattern is considered recognizable. The process is repeated for smaller and smaller bars, until HPA drops below the threshold.

3.3. MTF threshold

Qiu et al in their simulation [11] use electron tracing to estimate the *point spread function* (PSF) of an IIT. From PSF, they calculate the *line spread function* (LSF). The Fourier transformation of LSF gives MTF. Then, they use threshold value to obtain resolution from MTF. For them, resolution is equal to spatial frequency which produces MTF equal to a certain value.

The end user rarely has access to internal parameters of an IIT needed for electron tracing. Cathode voltage or MCP spacing are seldom stated in IIT test reports and they are challenging to measure for potted tubes. There are other methods to calculate MTF such as analysis of images of line or edge targets. Regardless the method, once MTF is obtained, the conversion to resolution is straightforward. Limited resolution is defined as the spatial frequency for which the MTF value is equal to the threshold.

3.4. Method comparison

The authors have tested resolution on a sample of eight IITs with methods presented in the previous sections and compared obtained results to ones generated by the classical subjective method. In the latter case, in order to increase repeatability, the resolution has been calculated as an average from several measurements using resolution patterns at different locations and different angular rotations.

The tested IITs have been selected to realistically represent tubes offered on the international market: the tubes are from different manufacturers, have different phosphor screens, screen curvature, generation, resolution and *fixed pattern noise* (FPN) (Table 1). The latter parameter is crucial for this paper. It is understood here as a standard deviation of spatial distribution of screen luminance. The results for all methods are gathered in Table 2.

The performance criterion of IITs called the FOM (*Figure of Merit*) is calculated as a product of measured resolution and SNR. An IIT grade and its price are based on calculated FOM. Therefore, there is market pressure on high accuracy of resolution measurement.

The FOM of modern IITs can be as high as 2000 and its requirements are typically presented with a step of 200 [6, 7]. The grading gap of 200 points is equal to the change of one element in resolved USAF test for the highest grade (64 lp/mm). Manufacturers started to add in-between patterns to make sure that the observer correctly resolved resolution patterns [14]. In practice, to account for the repeatability of the observer at least two additional patterns are added in between the standard USAF the elements (Fig. 1b). This results in a step between elements of the modified resolution target equal to 3%. To keep the target consistent, the same 3% step is also used for other resolutions. Note that for classical method, the target step can be considered as method accuracy.

As can we see in Table 2, none of tested methods can offer accuracy below the required level. In detail, the average error offered by the MTF threshold method is only slightly below 3.0%,

Table 1. IITs characteristics.

Tube no.	Generation	Resolution (classical) [lp/mm]	FPN normalized to Tube no. 1 [–]	Phosphor type
1	2+	58.8	1.00	P20
2	2+	48.9	1.20	P20
3	3	66.2	0.81	P43
4	2+	55.5	1.10	P43
5	2+	54.6	1.32	P20
6	2+	64.2	1.38	P20
7	2+	68.7	1.00	P45
8	2+	81.0	1.10	P43

Table 2. Comparison of objective methods.

Method	Maximum relative difference from the classical method d_{max} $$d_{max} = \max \left| \frac{R_n - R_{n\text{classical}}}{R_{n\text{classical}}} \right|$$	Average module relative difference from the classical method d_{avg} $$d_{avg} = \frac{1}{n} \sum \left| \frac{R_n - R_{n\text{classical}}}{R_{n\text{classical}}} \right|$$
MOB	−6.5%	4.0%
Fourier transform of bar patterns	10.5%	4.5%
MTF threshold	4.9%	2.9%

but the maximum error is over one and a half times over the limit. Further on, the situation is much worse for the other two methods. Here, even an average module relative difference from the classical method is almost two times over the limit.

There is a possibility that the authors have not perfectly implemented the analysed methods. There is a chance that if original authors of these methods had carried out such tests, they could have obtained results of difference lower comparing to the classical method. However, in the opinion of the authors of this paper, the analysed methods cannot generate results of accuracy below 3.0%.

In addition, the methods presented here enable the measurement of only average resolution, while test teams are often interested in measuring maximum resolution (measurement at the so-called sweet spot). In such a situation a new method capable of offering better accuracy and ability to measure both average and maximal resolution should be developed.

4. Improved objective method – the CNR method

The analysis carried out by the authors has shown that the methods discussed in the previous chapter do not take into account the spatial noise of IITs. In the authors' opinion, it is the main reason for modest accuracy of these methods, as intensity of spatial noise varies significantly from one tube to another (Table 1). Figure 2 shows a comparison between two IITs with different FPNs.

The authors have decided to eliminate this drawback by adding a parameter that characterized spatial noise. In detail, it is proposed to use modified *contrast to noise ratio* (CNR) as a resolvability metric, with effective noise $\sigma_{\text{effective}}$ as a parameter to describe the influence of spatial noise on image quality perceived by human observers. Targets with CNR above the threshold are considered to be resolvable.
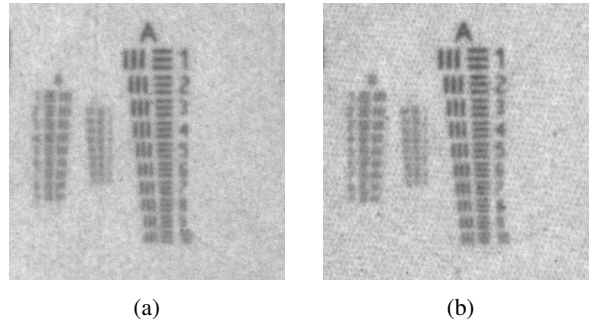
| (a) | (b) |

Fig. 2. Image from IITs with a) low and b) high FPN.

4.1. CNR definition

The impact of spatial noise on image quality is often expressed in terms of CNR which is defined [15] as in (4):

$$CNR = \frac{S_{\text{target}} - S_{\text{background}}}{\sigma_{\text{background}}} = \frac{\Delta S}{\sigma_{\text{background}}},$$ (4)

where: S_{target} – signal from the target, $S_{\text{background}}$ – signal from the background, $\sigma_{\text{background}}$ – standard deviation of image background noise.

CNR is a popular metric in field of medicine, especially in radiology where it is used to determine detectability of an object of interest such as a cyst or lesion [16–18]. Objects with a high contrast are easier to spot. Similarly, objects are easier to detect when there is little noise. When CNR is too low, the target can no longer be resolved.

Equation (4) describes the property of the image. However, in the case of resolution measurement, the image is evaluated by a human observer. The human eye has the unique property of filtering the image noise based on the observed target spatial frequency [19]. Additionally, as the target frequency increases (the bars are getting smaller), their contrast decreases starting from base contrast ΔS_0 for very large bars. The decrease in contrast is proportional to MTF.

Taking these two phenomena into consideration, we can rewrite (4) into a form suitable for IIT resolution (5).

$$\text{CNR}_{\text{IIT}}(\nu_{\text{IIT}}) = \frac{S_{\text{target}}(\nu_{\text{IIT}}) - S_{\text{background}}(\nu_{\text{IIT}})}{\sigma_{\text{effective}}(\nu_{\text{IIT}})} = \frac{\Delta S_{\text{IIT}}(MTF)}{\sigma_{\text{effective}}(\nu_{\text{IIT}})}.$$ (5)

Change the denominator from $\sigma_{\text{background}}$ to $\sigma_{\text{effective}}$ and its dependency on target spatial frequency ν_{IIT} indicates taking the observer into account. Target spatial frequency ν_{IIT} is defined in the photocathode plane. S_{target} and $S_{\text{background}}$ are signals coming from the bars and gaps between the bars respectively, as shown in Fig. 3. The next sections shows in detail how to calculate contrast and effective noise for a given target frequency.

We can use (5) to define resolution. Resolution R_{average} is a such spatial frequency of a resolution target for which CNR_{IIT} is equal to a threshold T_{CNR}, as in (6). Threshold T is found experimentally and is the same for all IITs.

$$\text{CNR}(R_{\text{average}}) = T_{\text{CNR}}$$ (6)

Note that CNR does not include target size. In general, up to a certain point, it is easier to spot a larger target. The same is true for brightness. Dimmer targets are more difficult to resolve. Fortunately, the measurement of resolution is a unique case, where the observer can adjust the light
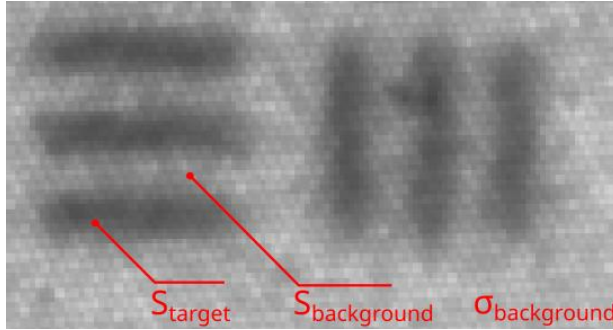
Fig. 3. Medium contrast image of a resolution pattern.

level and target size for best possible conditions. In the past, with analogue devices, it was done by varying microscope objective magnification M, aperture number $F\#$ and input light. Nowadays, with a video microscope, it is facilitated, as microscope gain G_{mic} and display luminance G_{disp} can be adjusted as well. As such, all targets, regardless of their initial spatial frequency v_{IIT} and brightness L_{IIT}, can be magnified and displayed at the same, best for observation, angular frequency v_{observer} and screen brightness L_{observer}, as in (7) and (8).

$$v_{\mathrm{observer}} = v_{\mathrm{IIT}} \cdot M_{\mathrm{mic}}\left(v_{\mathrm{IIT}}\right), \tag{7}$$

$$L_{\mathrm{observer}} = L_{\mathrm{IIT}} \cdot G_{\mathrm{mic}}\left(L_{\mathrm{IIT}}\right) \cdot G_{\mathrm{disp}}\left(L_{\mathrm{IIT}}\right). \tag{8}$$

Since both v_{observer} and L_{observer} are the same for all target spatial frequencies, we can omit their impact when modelling the resolution measurement.

To summarize, the authors have proposed to measure resolution using the method pipeline shown in Fig. 4.
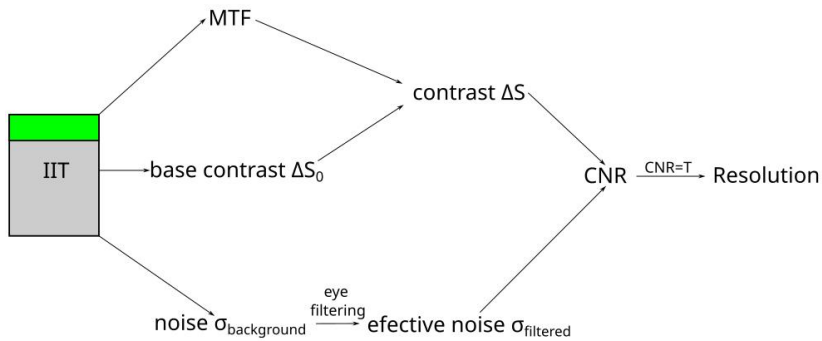

Fig. 4. CNR method pipeline.

4.2. Contrast ΔS_{IIT}

As the bars become smaller, so is getting the difference ΔS between the S_{target} and $S_{\mathrm{background}}$. We can predict this difference using MTF. MTF describes the contrast of sine wave targets and, in resolution testing, we are working with bar targets. MTF is well established and routinely measured. The *contrast transfer function* (CTF) is similar to MTF, but it describes the bar target

contrast. Typically, CTF is not measured in the case of IITs. Fortunately, for high frequency targets close to resolution limit, conversion from MTF to CTF is straightforward (6).

$$\text{CTF}(v) \approx \frac{4}{\pi} \cdot \text{MTF}(v). \tag{9}$$

Both MTF and CTF use the Michelson contrast $C_{\text{Michelson}}$ and, to calculate ΔS, we need to know the Weber contrast C_{Weber}. To convert $C_{\text{Michelson}}$ to C_{Weber}, we can use conversion coefficient k. The conversion coefficient is defined as (10):

$$k\left(C_{\text{Michelson}}\right) = \frac{C_{\text{Weber}}}{C_{\text{Michelson}}} = \frac{2}{1 + C_{\text{Michelson}}}. \tag{10}$$

Since MTF and CTF are normalized to zero spatial frequency, we also need to know contrast ΔS_0 at that frequency. Zero spatial frequency, in practice, means a sufficiently large target, such as the ones used during MTF measurements with an edge target. In laboratory conditions, when using a video microscope, the background signal $S_{0\text{background}}$ is usually set to the same level regardless of the gain of IIT for best repeatability. Once MTF and base contrast are known, it is possible to estimate contrast for other frequencies using (7)

$$\Delta S(v) = \frac{4}{\pi} \cdot \Delta S_0 \cdot k\left(\text{MTF}\right) \cdot \text{MTF}(v). \tag{11}$$

It should be noted that accurate measurement of MTF of IITs is challenging due to presence of spatial noise. As different techniques of MTF measurement can produce slightly different results [20], to reduce this problem, [21] shows that fitting a certain function to ESF data can give good, smooth MTF approximation even in the presence of noise.

4.3. Effective noise $\sigma_{\text{effective}}$

Measurement of resolution of IITs can be classified as a task of detection of a target on a noisy background. There have been several models proposed to predict the noise impact on the detection of target of interest located against a noisy background [19, 23, 24]. The authors have decided to use the work of Barten [19], who proposed an eye detection model in the form of internal noise and external noise. Internal noise, described by standard deviation σ_{internal}, stems from all the biological signal processing in the eye and brain. External noise σ_{external} is the noise from the observed image. Effective noise $\sigma_{\text{effective}}$ is geometrically the sum of those noises, as in (8).

$$\sigma_{\text{effective}} = \sqrt{\sigma_{\text{external}}^2 + \sigma_{\text{internal}}^2}. \tag{12}$$

For a high-light input signal when photon noise can be omitted, internal noise can be considered proportional to the input signal with proportional coefficient m (13). Barten estimated m for the internal noise (neural noise) to be 2.3%. We have experimentally estimated σ_{internal} and found out that for testing IITs a slightly higher m equal to 2.9% better fits to data.

$$\sigma_{\text{internal}} = m \cdot S_{0\text{background}} \tag{13}$$

External noise comes from FPN of the tested IIT. In the case of spatial noise, the eye performs the filtering based on the observed target spatial frequency v_{target}. Equation (14) shows the filter function Ψ and the shape of filter for different target frequencies is shown in Fig. 5. To apply the

filter function, noise needs to be decomposed into spectral components using power spectrum density. Equation (10) shows decomposition using power spectrum density Φ_{IIT}

$$\Psi = 0.747 \cdot \exp\left[-2.2 \cdot \ln^2\left(\frac{v_n}{v_{\text{target}}}\right)\right], \tag{14}$$

where v_n – noise spatial frequencies.

$$\Phi_{\text{IIT}}(v_n) = F(v_N)^2, \tag{15}$$

where F is a Fourier Transform of an image from IIT with a uniform target (Fig. 5d) and with the mean value removed. Power spectral density shows the variance of IIT screen luminance for a given spatial frequency. The square root of their sums gives $\sigma_{\text{background}}$.

$$\sigma_{\text{background}} = \sqrt{\int \Phi(v_n)\, \mathrm{d}v_n}. \tag{16}$$

Equation (17) shows how to obtain external noise calculated from the filter function and PSD_{IIT}. Note that external noise can be different for different target frequencies.

$$\sigma^2_{\text{external}}(v_{\text{target}}) = \int \Phi^2_{\text{IIT}}(v_n) \cdot \Psi(v_u, v_{\text{target}})\, \mathrm{d}v_n \tag{17}$$
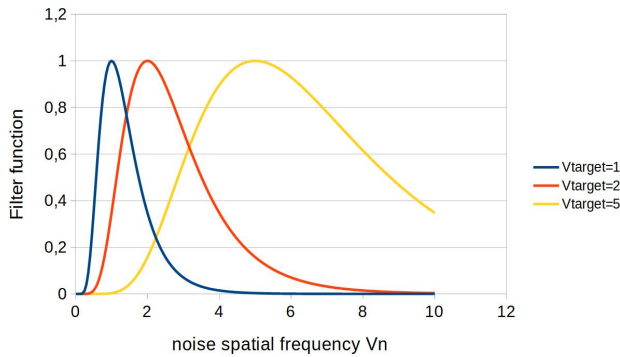

Fig. 5. Barten spatial filter for different target spatial frequencies v_{target}.

4.4. Maximum resolution

The resolution calculated using (6) corresponds to average resolution for the classical method. By average resolution we mean results from different positions of the target averaged. That is because MTF is calculated from a relatively large area compared to the size of the resolution pattern. In addition, several edge positions are averaged to exclude the possibility of a badly fitted ESF. The noise is also calculated as an average representation. For any IIT, it is possible to find the places where spatial noise is much smaller than the average.

To estimate maximum resolution, conversion coefficient k_{max}, is used as shown in (18). The tests have shown that maximum resolution is about 6% ($k_{\text{max}} = 1.06$) higher than average resolution. Figure 6 shows a comparison between average and maximum resolution for 3 observers using the classical method.

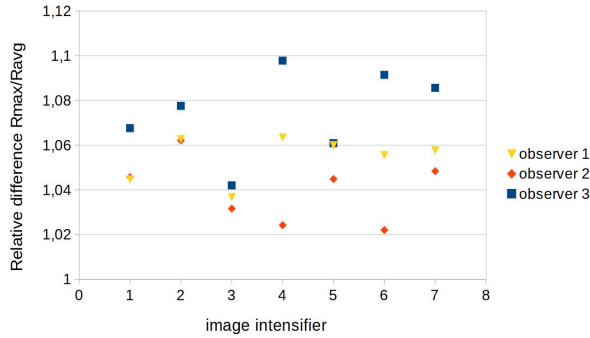$$R_{\text{max}} = k_{\text{max}} \cdot R_{\text{average}} \tag{18}$$

Fig. 6. Relative difference between maximum and average resolution for 3 observers using the classical method.

5. Experimental verification of the CNR method

5.1. Comparison with the classical measurement

The same IITs (Table 1) as in Section 3.4, have been tested on ITIP test station [14]. Test station is shown in Fig. 7. In order to measure MTF, a 1.5x1mm rectangle has been used with results from 5 different edge orientations averaged. All the measurements have been performed with the same background signal $S_{0background}$ equal to 200DN. Both detection threshold and internal noise constant have been determined experimentally.

The detection threshold has been estimated to be CNR = 0.9 and internal noise to $\sigma_{internal} = 5.8$ (2.9% of S_0 background). This is in good agreement with literature [25]. Typically, for a single pixel, the detection threshold for CNR is equal to 1. For larger structures, as is the case with the bar pattern, it can be slightly lower. Resolution results for those values are shown in Table 3.
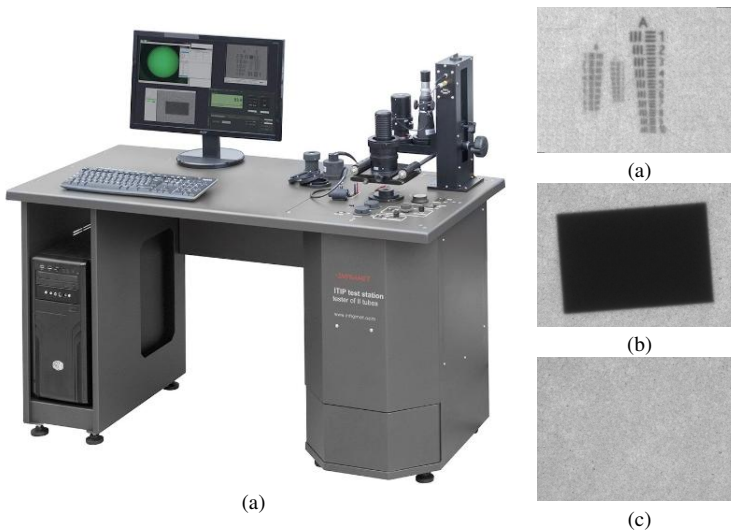

Fig. 7. a) ITIP test station, b) resolution target, c) edge target, d) uniform target. Target images taken from the measurements.

Looking at Table 3, one can notice there is good agreement between predicted and measured resolution. The difference between the classical and CNR method is at an acceptable level: errors for all cases, including the maximum deviation, are below the level of 3.0%.

Table 3. Comparison between classical and CNR measurements of average resolution.

Intensifier no.	CNR method resolution [lp/mm]	Classical method resolution [lp/mm]	Difference [lp/mm]	Relative difference [%]
1	57.0	58.8	1.3	-2.3
2	49.0	48.9	0.1	0.2
3	65.0	66.2	1.2	-1.9
4	55.0	55.5	0.5	-1.0
5	56.0	54.6	1.4	2.6
6	65.0	64.2	0.8	1.2
7	69.5	68.7	0.8	1.2
8	80.0	81.0	1.0	1.2

The repeatability of the CNR has been measured and compared to the standard measurement. Both methods yielded the same result of approximately 3%. The repeatability stems mostly from variance in MTF measurement. Figure 8. shows partial results for CNR and the standard method for IIT no 1.
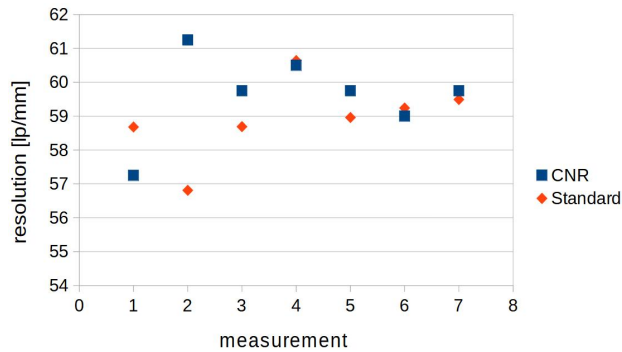

Fig. 8. Repeatability of the CNR method for IIT no 1.

The method is designed to measure average resolution. However, it can also be used to estimate maximum resolution with a slightly lower accuracy. The results for maximum resolution for conversion coefficient $k = 1.06$ are shown in Table 4.

Table 4. Comparison between standard and CNR measurements of maximum resolution.

Intensifier no.	CNR method resolution [lp/mm]	Classical method resolution [lp/mm]	Difference [lp/mm]	Relative difference [%]
1	61	62.2	1.1	1.9
2	51.9	52.3	0.4	-0.7
3	68.9	68.7	1.2	-0.3
4	58.3	58.9	0.7	-1.0
5	59.4	57.7	1.7	2.9
6	68.9	67.9	1.0	1.5
7	73.7	73.3	0.4	0.6
8	84.8	85.8	1.0	-1.2

The average difference for maximum resolution is still small, but maximum difference is slightly larger. This is expected, since maximum resolution is a very localized and individualized parameter. The model is estimating maximum resolution based on average from a large pool of IITs, which can only give a general estimation. Yet, despite these limitations, the highest difference is still within the set limit.

5.2. Comparison to other objective methods

Table 5 shows a comparison of methods discussed in Section 3 As predicted, incorporation of spatial noise into the model improved the prediction power. Both maximum difference and standard deviation are lowered.

Table 5. Comparison between CNR and other objective methods.

Method	Maximum relative difference from the classical method d_{max} $d_{max} = \max\left\|\dfrac{R_n - R_{n\text{classical}}}{R_{n\text{classical}}}\right\|$	Average module relative difference from the classical method d_{avg} $d_{avg} = \dfrac{1}{n}\sum\left\|\dfrac{R_n - R_{n\text{classical}}}{R_{n\text{classical}}}\right\|$
MOB	6.5%	4.0%
Fourier transform of bar patterns	10.5%	4.5%
MTF threshold	4.9%	2.9%
CNR	2.6%	1.8%

6. Conclusions

This paper presents a new method for objective measurement of resolution of image intensifier tubes that offers significantly better accuracy compared to the previously developed measurement methods. The improved accuracy has been achieved by using a mathematical model that takes into account the influence of spatial noise effect on human perception of image of the resolution target during the measurement process.

The method has been verified by a direct comparison with the standard approach based on human observer. The test results are in good agreement for both average and maximum resolution values. The repeatability of the method is on the same level as the standard subjective measurement.

This new approach improves the accuracy of measurement of resolution of IITs to a level that can be accepted at professional test stations. Thus. this new method has potential to replace the standard subjective method to measure resolution of IITs and fix the biggest flaw of the standard test stations: measurement subjectivity.

References

[1] Chrzanowski, K. (2013). Review of night vision technology. *Opto-Electronics Review*, *21*(2), 153–181. https://doi.org/10.2478/s11772-013-0089-3

[2] Bosch, L. A. (2000, November). Image intensifier tube performance is what matters. In *Image Intensifiers and Applications II* (Vol. 4128, pp. 65–78). SPIE. https://doi.org/10.1117/12.405867

[3] MIL-I-49428(CR). (1989). Military specification: Image Intensifier Assembly, 18 mm, Microchannel Wafer MX-10160/AVS-6.

[4] MIL-PFG-4940F. (1999). Performance Specification Image Intensifier Assembly 25 Millimeter, Microchannel Inverter MX-9644/UV.

[5] MIL-I-49052F. (1990). Military specification: Image Intensifier assembly, 18 mm, Microchannel Wafer MX-9916/UV

[6] Photonis. (n.d.). *Image intensifier tube ECHO.* https://www.photonis.com/products/image-intensifier-tube-echo

[7] Photonis. (n.d.). *Image intensifier tube 4G.* https://www.photonis.com/products/image-intensifier-tube-4g

[8] HARDER digital. (n.d.). *Generation II Image Intensifiers.* https://harderdigital.com/products/#generation_image_intensifiers

[9] Stefanik, R. (1994). *Image intensifier system resolution based on laboratory measured parameters* [Technical Report No. 0112]. Night Vision and Electronic Sensors Directorate, Fort Belvoir.

[10] Wang, L., Qian, Y., & Wang, H. (2020). Objective evaluation of the resolution of low-light-level image intensifiers based on fast Fourier transform. *Optical Engineering*, *59*(05), 1. https://doi.org/10.1117/1.oe.59.5.054106

[11] Qiu, Y.-F., Yan, W.-L., Hua, S.-T. (2020). Resolution research of low-light-level image intensifier based on electronic trajectory tracking. *Acta Photonica Sinica*, *49*(12), 19–26. https://doi.org/10.3788/gzxb20204912.1223003 (in Chinese)

[12] Chrzanowski, K. (2015). Review of night vision metrology. *Opto-electronics Review*, *23*(2). https://doi.org/10.1515/oere-2015-0024

[13] MIL-STD-150A. (1959). Military standard: Photographic lenses.

[14] INFRAMET. (n. d.). *ITIP test station.* https://www.inframet.com/Data_sheets/ITIP.pdf

[15] *Contrast-to-noise ratio* (2024, March 5). In *Wikipedia.* https://en.wikipedia.org/wiki/Contrast-to-noise_ratio

[16] Nett, B. (2022). *X-ray Contrast to Noise (CNR) Illustrated Examples of Image Noise (SNR, Quantum Mottle) for Radiologic Technologists.* How Radiology Works. https://howradiologyworks.com/x-ray-cnr/

[17] Palmer, M., & Benbow, M. (n.d). *Contrast to Noise Ratio (CNR).* http://www.bamrr.org/wp-content/uploads/2019/11/Bitesized-Physics-Contrast-to-Noise-Ratio.pdf

[18] Wang, F., Xie, X., Li, G., & Zhang, Z. (2020). Relationship between CNR and visibility of anatomical structures of cone-beam computed tomography images under different exposure parameters. *Dentomaxillofacial Radiology*, *49*(5), 20190336. https://doi.org/10.1259/dmfr.20190336

[19] Barten, P. G. J. (1999). Contrast sensitivity of the human eye and its effects on image quality. In *SPIE eBooks.* https://doi.org/10.1117/3.353254

[20] Ortíz, S., Otaduy, D., & Dorronsoro, C. (2004). Optimum parameters in image intensifier MTF measurements. *Proceedings of SPIE.* https://doi.org/10.1117/12.578066

[21] Barney Smith, E. H. (2006). PSF estimation by gradient descent fit to the ESF. *Proceedings of SPIE.* https://doi.org/10.1117/12.643071

[22] Li, T., Feng, H., Xu, Z., Li, X., Cen, Z., & Li, Q. (2009). Comparison of different analytical edge spread function models for MTF calculation using curve-fitting. *Proceedings of SPIE.* https://doi.org/10.1117/12.832793

[23] Roka, A., Galambos, P., & Baranyi, P. (2009). Contrast sensitivity model of the human eye. In *4th International Symposium on Computational Intelligence and Intelligent Informatics (ISCIII)*. IEEE. https://doi.org/10.1109/isciii.2009.5342274

[24] Robson, J. G. (1966). Spatial and temporal Contrast-Sensitivity functions of the visual system. *Journal of the Optical Society of America*, *56*(8), 1141. https://doi.org/10.1364/josa.56.001141

[25] Hamamatsu Photonics (n.d.). *CNR (Contrast-to-Noise Ratio), eye versus machine*. https://camera.hamamatsu.com/jp/en/learn/technical_information/thechnical_guide/contrast.html

Krzysztof Chrzanowski received his Ph.D., and D.Sc. both in electronics, from the Military University of Technology in Warsaw, Poland. He works currently as Professor of the same university. His main scientific interests include system analysis, characterization, testing and computer simulation of electro-optical surveillance systems (thermal imagers, night vision devices, VIS-NIR cameras, SWIR imagers, laser range finders, laser designators, fused imagers, multi-sensor surveillance systems). He is an author or co-author of over 150 scientific papers and conference communications. He is also the CEO of a high-tech company that manufactures equipment for testing electro-optical imaging and laser systems (Inframet, www.inframet.com).

Bolesław Stafiej received his B.Sc. in photonics from Warsaw University of Technology. His main scientific interests include image intensifier systems, mostly used in night vision technology and solar blind cameras. Since 2016, he has worked at the R&D department of Inframet, a high-tech company that manufactures equipment for testing electro-optical imaging and laser systems.